


## Article

# Destabilization Mechanism and Stability Study of Collapsible Loess Canal Slopes in Cold and Arid Regions

Haozhen Xu <sup>1,2</sup>, Lingkai Zhang <sup>1,2,\*</sup>  and Chong Shi <sup>1,2,3</sup>

<sup>1</sup> College of Water Resources and Civil Engineering, Xinjiang Agricultural University, Urumqi 830052, China; xjauhz@163.com (H.X.); scvictory@hhu.edu.cn (C.S.)

<sup>2</sup> Xinjiang Key Laboratory of Water Conservancy Engineering Safety and Water Disaster Prevention and Control, Urumqi 830052, China

<sup>3</sup> Geotechnical Research Institute, Hohai University, Nanjing 210098, China

\* Correspondence: xjauzhanglk@163.com

**Abstract:** The combination of seasonal shutdowns, water conveyance, cold, and drought can easily lead to the deterioration of the anti-seepage system and loess foundation of the canal, which contributes to the destruction of the slope. To reveal the failure mechanism of the collapsible loess canal slope, this paper is based on the results of laboratory tests and adopts numerical simulations to analyze the stability of the canal slope under different conditions. The results show that the shear strength indexes and elastic modulus *E* of loess decrease following an exponential pattern with the increase in wetting-drying and freezing-thawing (WD-FT) cycles. The height of the seepage overflow point yields little effect on the water level behind the impermeable membrane, whereas the height of the water level has a significant effect. In the operation period, the slope under any working conditions is in a relatively stable state. However, the slope with a water level of 4.5 m behind the impermeable membrane tends to be unstable after three WD-FT cycles during the shutdown period. By replacing the surface-degraded loess with sand gravel and picking a depth of 0.9–1.2 m, the slope will maintain a long-term stable state.

**Keywords:** cold and arid regions; collapsible loess; water conveyance canal; sliding failure; stability analysis



**Citation:** Xu, H.; Zhang, L.; Shi, C. Destabilization Mechanism and Stability Study of Collapsible Loess Canal Slopes in Cold and Arid Regions. *Appl. Sci.* **2024**, *14*, 4518. <https://doi.org/10.3390/app14114518>

Academic Editor: Tiago Miranda

Received: 24 April 2024

Revised: 17 May 2024

Accepted: 21 May 2024

Published: 24 May 2024



**Copyright:** © 2024 by the authors. Licensee MDPI, Basel, Switzerland. This article is an open access article distributed under the terms and conditions of the Creative Commons Attribution (CC BY) license (<https://creativecommons.org/licenses/by/4.0/>).

## 1. Introduction

Loess is a yellow, homogeneous quaternary silt deposit that blankets vast tracts of land. It is found mainly in the arid and semi-arid regions of the northern hemisphere at mid-latitudes, including Asia, Europe, and the mid-western United States [1,2]. Among them, China is the country with the widest distribution and greatest thickness of loess in the world, with a distribution area of more than 640,000 km<sup>2</sup>, accounting for about 6.6% of the land area of the country. Loess is mainly concentrated in the northwestern, northern, and northeastern regions of China [3,4]. Loess has special engineering properties such as porosity, a loose structure, and strong water sensitivity. Under the combined action of flooding and overlying pressure, the loess structure is rapidly destroyed and is prone to significant collapsibility deformation [5,6]. Therefore, engineering hazards are very prominent in the cold and arid regions of Northwest China where the natural environment is relatively harsh [7]. The extensive network of water transfer canals in Xinjiang, China, including a section of canal that passes through the collapsible loess region, is affected by the unique natural environment and seasonal water supply mode of the region. Seepage issues and the damages caused by canal slope destabilization have severely hampered the effectiveness of the water transfer and safe operation of the canal projects.

To date, many scholars have carried out research on the strength characteristics of loess under wetting-drying (WD) cycles [8] and freezing-thawing (FT) cycles [9]. Numerous findings indicate that increasing the number of WD cycles and cyclic amplitude generally

lead to the development of irregular cracks within loess, increased permeability, significantly decreased cohesion and angle of internal friction of the soil, and severe deterioration of the shear strength [10,11]. During FT cycles, the fragmentation and reorganization of loess particles lead to structural damage, and the development of internal pore space in the soil. With increasing cycles, the loss of the peak strength of loess gradually increases, and the shear strength continues to decrease and eventually approaches a residual value [12,13]. Due to extreme cold and abnormal drought, loess in Northwest China is always under the coupling action of alternating dry and wet and repeated freeze–thaw cycles. The long-term WD-FT cycles result in the deterioration of the physico-mechanical properties of loess, and the cracks on the soil surface intensify, which in turn induces a series of engineering problems, such as foundation settlement and slope instability [14,15].

Under the WD-FT cycles, the deterioration of the soil and the action of water also have certain effects on slope stability [16]. However, the water conveyance facilities represented by the canal are inherently characterized by water flow and unloading [17]. Thus, the canal projects are more prone to slope instability under the coupled action of the WD and FT cycles. In view of this fact, a number of field studies [18,19], physical model tests [20,21], and numerical simulations [22,23] have been carried out on in-depth investigations of the mechanism and instability damage of canal slopes. Rahimi et al. statistically evaluated the development law of the cracks and the influencing factors. The sliding damage of expansive soil canal slopes was mostly contributed to by various kinds of cracks [24,25]. Zhu et al. studied the water infiltration characteristics of the canal under various cyclic conditions with centrifuge model tests and demonstrated that the shallow soil of the canal model was completely saturated in the wetting stage [26]. Jamsawang et al. analyzed the stability of the slope of the soft clay drainage channel through field testing and the finite element method. It is believed that the time-varying and undrained creep behavior of extremely soft clay was suspected to be the cause of the canal rupture [27]. Karmakar et al.'s previous studies have shown that the slope stability of a canal embankment depends on the geometry of the side slopes, in situ soil condition, and effects of excess pore water pressure [28]. Deng et al. analyzed the stability of the expansive soil slope in northern Xinjiang and proposed a series of improvement measures, such as replacing the surface layer of the deteriorated soil, and installing additional seepage pumping facilities [29,30].

In summary, the deterioration of soil at the base and water infiltration adversely affected the stability of the canal slopes, and WD-FT cycles will also exacerbate the sliding damage of the slope. The current studies on the sliding damage mechanism of canal slopes have mainly focused on expansive soils, but there have been fewer studies on collapsible loess canal slopes under the WD-FT cycles. Given this, this paper takes a water conveyance canal in Xinjiang [31] as the research object. The deterioration law of the mechanical properties of loess under the WD-FT cycles is analyzed based on laboratory tests. The influence mechanism of the canal seepage is explored by using Geo-Studio 2020 (SEEP/W) [32] seepage analysis software, and the stability of the canal slope is comparatively analyzed with the software FLAC3D 6.00.69 [33]. The study is of great significance in that it provides a theoretical basis and technical support for the operation, maintenance, risk removal, and reinforcement of collapsible loess canal slopes.

## 2. Materials and Methods

### 2.1. Project Overview

The study area is located in the mid-latitude plains and has a temperate continental arid climate [34]. The surface temperature in summer exceeds 40 °C, and in winter, the surface temperature is as low as −20 °C. Rainfall is low and the water table is deep. The section of the canal is trapezoidal in shape, with a slope height of 6 m. The inner ratio of the canal is 1:2.0, and the thickness of the lining structure is 12 cm, with a 50 cm thick gravel bedding layer underneath the lining structure. The soil layers below the bedding layer are all collapsible loess [35,36]. To reduce frost damage to the canal lining structure, a seasonal

water conveyance scheme is adopted, i.e., the water conveyance starts in spring and stops in fall every year.

Geological conditions along the canal project are complicated, and one of the significant influencing factors on the canal is the collapsible loess [31,37]. The canal section located in the loess region accounts for about 19% of the total length of the canal. The loess in this section is mostly porous loess with poor quaternary accumulation cohesion. The soil particles are uniform with developed vertical joints. The color is gray to yellow with medium humidity. Over the years of operation of the canal project, the canal has suffered from severe localized seepage, and sliding damage to the canal slope has occurred many times. In response to this engineering problem, the canal management agency modified the section of the canal that passes through the loess region. The top layer of the loess was replaced with gravel to mitigate the settlement deformation of the canal [38] and to reduce the negative impacts of salt expansion and frost heave. It is one of the most used methods with simple access to materials and convenient construction organization.

By conducting the water content test, density test, particle analysis test, limiting water content, and compaction test on the loess of the canal foundation, the basic physical properties of the loess were determined as summarized in Table 1.

**Table 1.** Basic physical properties of collapsible loess.

Soil Sample	Granulometric Composition/mm				
	>0.075		0.075~0.005		<0.005
collapsible loess	0.6		83.1		16.3
Natural Dry Density	Natural Water Content	Liquid Limit	Plastic Limit	Optimum Moisture Content	Maximum Dry Density
1.56 g/cm <sup>-3</sup>	11.10%	27.92%	15.24%	15.10%	1.74 g·cm <sup>-3</sup>

2.2. Direct Shear Test of Loess under WD-FT Cycles

During the operation of the canal, the loess at the base of the canal undergoes WD and FT cycles simultaneously. Before the implementation of the WD-FT cycle test, the boundary conditions were first set, as presented in Table 2. Then, a series of laboratory direct shear tests were performed on the specimens with various WD-FT cycles to determine the change rule of the mechanical parameters of the loess. The ZJ50-1A type strain-controlled direct shear instrument was used to carry out consolidated quick shear tests on the specimens with different cycles to obtain the change rule of the strength parameters of the loess. The test process is shown in Figure 1.

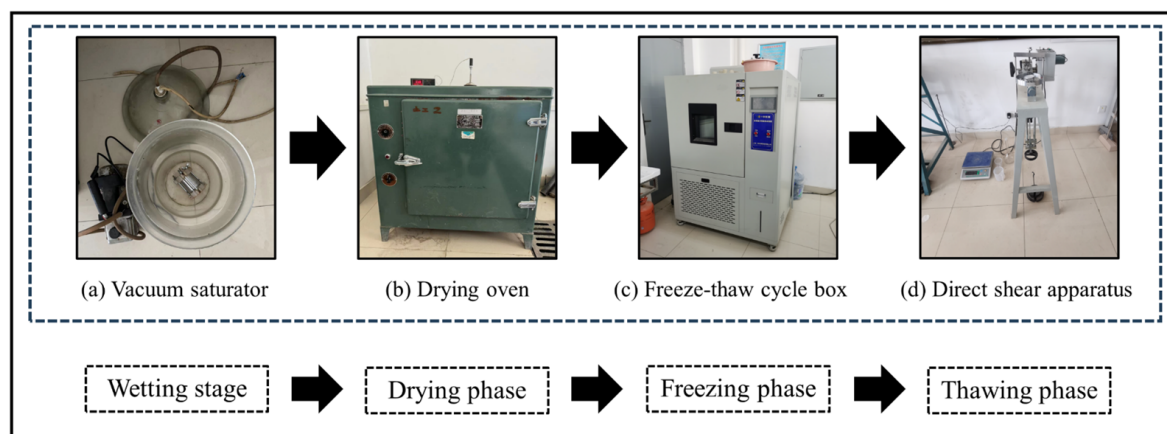


**Figure 1.** Direct shear test under WD-FT cycles.

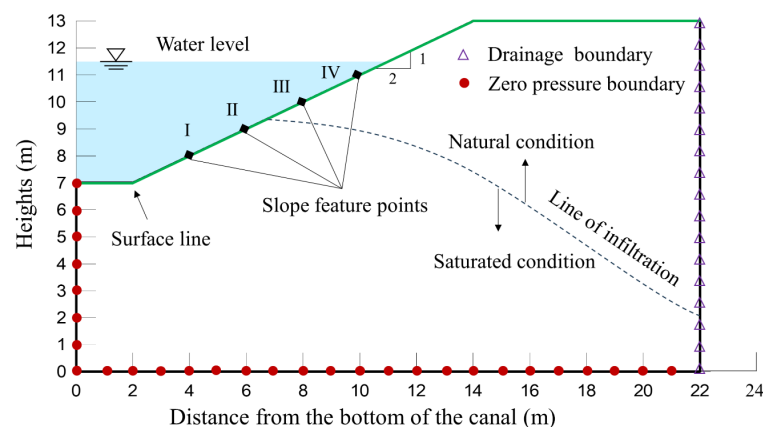
**Table 2.** WD-FT cycle test boundary setting.

State	Wet	Dry	Freeze	Thaw
Temp/°C	Ordinary temp	40	−20	20
Time/h	Saturated 12 h	12 h, To $\omega_D$	12	12
Cycle/times	9	9	9	9

### 2.3. Analysis of the Influence of Seepage on Collapsible Loess Slope

Over the years of canal operation, the aging of impermeable materials and uneven settlement of the canal base have created different degrees of damage to the impermeable system. The monitoring results of seepage flow confirm that the canal seepage is serious [39], which poses a threat to the safety and stability of the canal slopes. The water level behind the impermeable membrane develops gradually with the seepage in the canal. Since the study area is located on the plains in the typical cold and arid region of Northwest China, with relatively less rainfall and deeper buried groundwater along the canal, canal seepage is the main source of the water behind the membrane.

The SEEP/W module in Geo-Studio 2020 was used to simulate the steady-state seepage of the canal. The influence mechanisms of different heights of the seepage overflow point and water levels during the operation period on the change in the infiltration line and pore water pressure of the canal slope were analyzed. To simplify the model, groundwater and rainfall boundary conditions were not considered. The top, bottom, and left boundaries of the model were set as zero-flow boundaries, while the slope side and right boundaries of the canal were set as permeable boundaries. The simplified cross-section of the canal is shown in Figure 2.

**Figure 2.** Typical canal profile during the water conveyance period.

### 2.4. Stability Analysis of Collapsible Loess Slope

To investigate the stability of the canal under the action of the WD-FT cycle and water seepage, a three-dimensional simplified model of the canal was constructed using FLAC3D 6.0, and half of the canal slope profile was selected for stability calculation. The canal model is illustrated in Figure 3, where the  $x$ -axis indicates the transverse direction of the canal with a calculated width of 22 m, the  $y$ -axis indicates the longitudinal direction of the canal with a calculated length of 30 m, and the  $z$ -axis indicates the direction of the canal height with a calculated length of 13 m. The thickness of the soil at the base of the canal is 7.0 m, and the height of the canal slope is 6.0 m.

A Mohr-Coulomb elastoplastic model was adopted for the stability analysis of the canal slopes, and the strength reduction method was also used in the numerical model [40]. The core of the strength reduction method is to use the reduction coefficient  $F_{trial}$  on the soil body of the shear strength index cohesion  $c$  and the angle of internal friction  $\varphi$  for the reduction, and after the reduction in the parameter indicators use these again on the stability of the slope for numerical analysis. Then increase the reduction coefficient until



the slope reaches the critical damage at this time, the original cohesion, and the reduction in the ratio of the cohesion at the time of the critical damage, which is the coefficient of safety. The basic formula of the strength reduction method is:

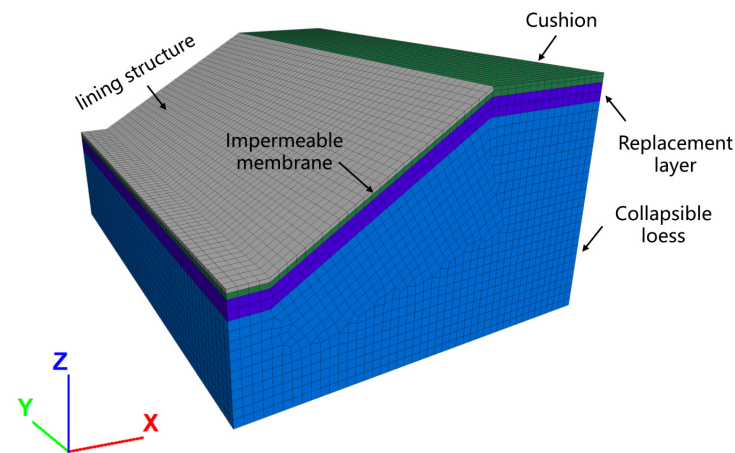


**Figure 3.** Model of the collapsible loess canal.

$$c_F = c_0 / F_{trial} \quad (1)$$

$$\tan \varphi_F = \tan \varphi_0 / F_{trial} \quad (2)$$

where  $F_{trial}$  is the reduction factor;  $c_0$  is the cohesion before reducing;  $\varphi_0$  is the angle of internal friction before reducing; and  $c_F$  is the cohesion and internal friction angle of the slope when it reaches the critical failure state, respectively.

According to the “Water Conservancy and Hydropower Engineering Slope Design Specification” [41], the canal slope is divided into the following five grades by taking the  $F_s$  of the anti-slide stability of the canal slope as the evaluation criterion, and the specific stability divisions are presented in Table 3. As a key project of the water conveyance canal project in Xinjiang, China, the safe operation of the case canal will have a significant impact on the economy, environment, and society along the route, so the slope level of the canal is set as Grade 1 and the  $F_s$  of the canal slope should be higher than 1.25. For the Grade 1 slope, the strength reduction method can be used to check its anti-slide stability.

**Table 3.** Grading of slope stability.

Slope Grade	$F_s$
1	1.25–1.30
2	1.20–1.25
3	1.15–1.20
4	1.10–1.15
5	1.05–1.10

To prevent frost damage to the canal, the canal adopts a seasonal water conveyance method. The water conveyance canal is opened from mid-April to early October every year. Starting from mid-April, the water conveyance volume is gradually increased, and the water level in the canal reaches the operational level of 4.5 m after 15 days. According to the results of the water content monitored by the high-density electrical detection method [42], the water level behind the impermeable membrane of the canal slope is almost even with the bottom of the canal before the operation of the canal. A few days after the water conveyance, the water level behind the impermeable membrane rises, with a change varying from 0 to 4.5 m. To simplify the calculation, the soil on the canal slope below water level behind the impermeable membrane is set to be saturated, and this soil is assigned saturated weight, with the rest of the soil in its natural state.

The canal is out of operation from November to March of every year. Beginning in late October, the water level in the canal gradually decreases until it reaches the bottom of the canal, which takes about 15–20 days. Slowly lowering the water level can effectively reduce the disturbance effect of water level change on the canal slope, so the effect on the stability of the canal slope is negligible. The water level behind the impermeable membrane decreases as the water level in the canal gradually decreases. However, in November of each year, as winter approaches and the average daily temperature in the study area falls below 0 °C, the seepage water behind the membrane freezes before it has a chance to be set free, so the water behind the membrane remains at a high level.

### 3. Results

#### 3.1. Strength Characteristics of Collapsible Loess

The strength properties generally refer to the ultimate capacity of the soil to resist shear deformation under external loading. In the simulation analysis of the stability of canal slopes, the change in the modulus of elasticity of the loess at the base of the canal has an impact on the factor of safety and the displacements of the canal slopes [43]. Therefore, only considering the change in soil shear strength and ignoring the influence of the elastic modulus on the stability of canal slopes is not sufficient to reflect the practical situations of the canal slopes. Thus, it is necessary to consider both the soil shear strength and the elastic modulus at the same time.

Figure 4 shows the change curves of the  $c$ ,  $\varphi$ , and  $E$  of loess specimens with varying WD-FT cycles. As can be seen from Figure 4, the  $c$ ,  $\varphi$ , and  $E$  all exhibit a decreasing trend with the increasing WD-FT cycles, with the decay amplitude of the  $c$  being the largest and that of the  $\varphi$  being relatively lower. By fitting the data in Figure 4, it is concluded that the exponential function can well describe the influence of the number of WD-FT cycles  $N$  on the  $c$ ,  $\varphi$ , and  $E$  of loess. The fitted equations are as follows:

$$c = 10.21 + 11.31 \cdot e^{-N/2.06} \quad (3)$$

$$\varphi = 13.64 + 2.93 \cdot e^{-N/2.47} \quad (4)$$

$$E = 7.76 + 4.47 \cdot e^{-N/1.89} \quad (5)$$

where  $c$  is the cohesion;  $\varphi$  is the angle of internal friction;  $E$  is the modulus of elasticity; and  $N$  is the number of WD-FT cycles.

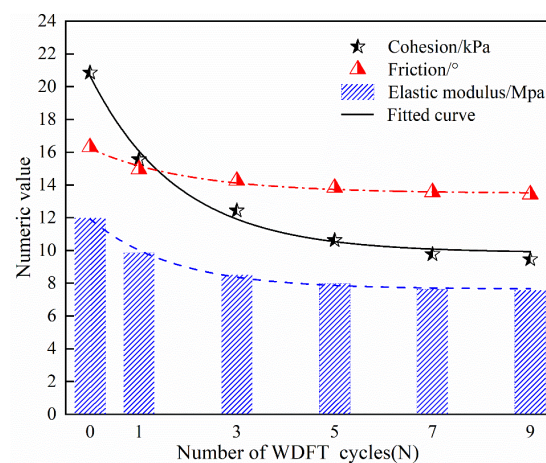


**Figure 4.** Variation in loess strength parameters with different WD-FT cycles.

The analysis of the stability of loess canal slopes that undergo different numbers of WD-FT cycles should fully consider the influence of the local environment. Meanwhile, the shear strength indexes and modulus of elasticity of loess should be reasonably reduced

according to Equations (3)–(5) to capture the actual deterioration process of loess at the base of the canal.

### 3.2. Influence Mechanism of Water Level behind the Impermeable Membrane

#### 3.2.1. Influence of Height of Seepage Overflow Point

To investigate the influence mechanism of the heights of the canal seepage overflow point on the change in water level behind the impermeable membrane, four kinds of seepage overflow point height tests were established. The blue arrows in the figure indicate the location of the seepage points. The heights of the seepage points were set to 1, 2, 3, and 4 m, respectively, and the operating water level was maintained at 4.5 m. The results of the seepage simulation on the canal slope are displayed in Figure 5.

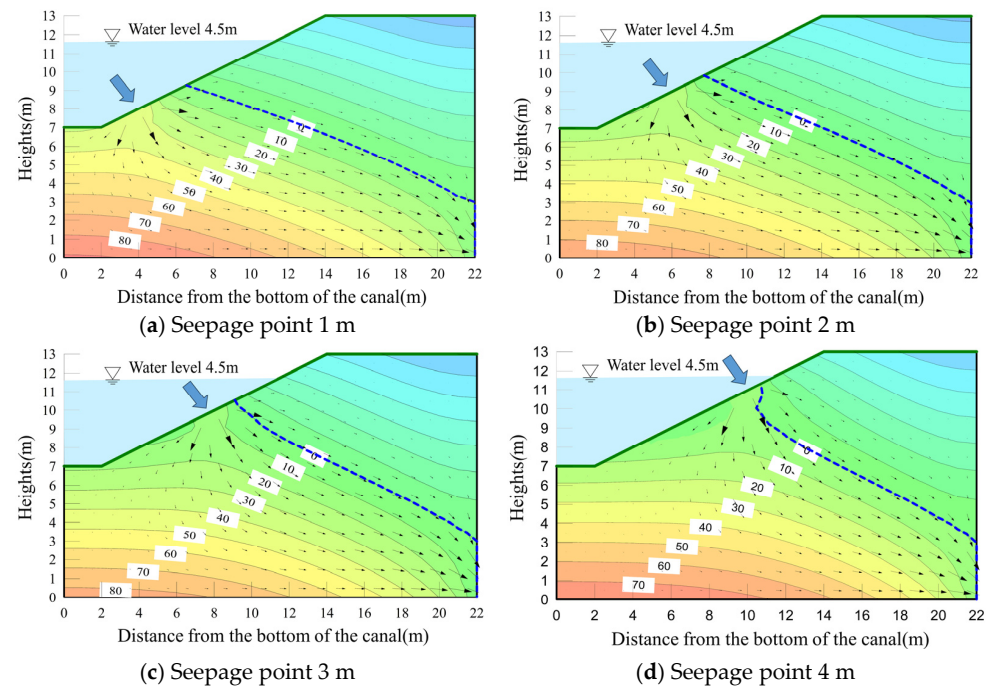


**Figure 5.** Nephograms of pore water pressure at different heights of the seepage overflow points.

As indicated in Figure 5, with the increase in the heights of the seepage overflow point, the infiltration lines of the canal slope gradually develop from the gentle feature at the feature points I and II on the slope surface to the curved feature at points III and IV, and then they maintain the same height at the escape point. The overall seepage paths are the same, and the distribution of pore water pressure below the infiltration line is uniform, with a range of 0–90 kPa, reflecting that the water level behind the impermeable membrane is about 4 m below the top surface of the canal. The simulated results are consistent with the results of the water content detected by the high-density electrical method [42]. This is because the pore water pressure at the feature points of the slope surface changes from the original unsaturated state to a saturated state, while it remains unchanged inside the canal slope.

#### 3.2.2. Influence of Water Level in the Operation Period

To investigate the influence mechanism of the heights of the water level in the operation period on the change in water level behind the impermeable membrane, four kinds of water level height tests were established. The heights of the water level were set to 1, 2, 3, and 4 m, respectively, and the height of the seepage point was maintained at 1 m. The seepage simulation results are displayed in Figure 6.

As can be seen from Figure 6, with the increase in the water levels in the operation period, the pore water pressure increases rapidly. The infiltration line then rises, resulting

in the water level behind the impermeable membrane of the canal slope rising to a higher level. This is because water infiltrates toward the upper part of the canal slope under the effect of soil matrix suction as a result of the continuous infiltration of canal water from the shallow water deep into the soil. It can be seen that there is a high correlation between the water level in the operation period of the canal and the water level behind the impermeable membrane.

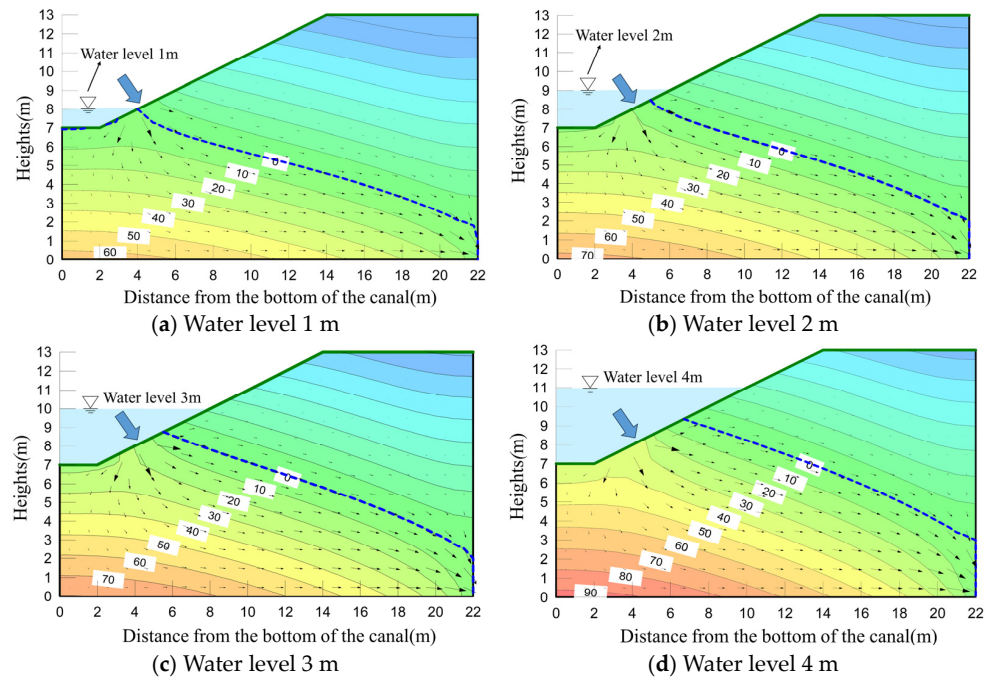


Figure 6. Nephograms of pore water pressure with different water levels in the operation period.

In summary, the influence of the seepage overflow point height on the change in the water level behind the impermeable membrane on the canal slope is relatively small, while the water level in the operation period of the canal significantly affects the water level behind the impermeable membrane. The water level behind the impermeable membrane rises with the increase in the water level in the operation period of the canal. The influence of the seepage overflow point height on the stability of the canal slope is ignored in the following finite element analysis, and only the influence of the change in water level in the operation period is considered. To simplify the calculation, the water level behind the impermeable membrane is set up to be 2 m above the base of the canal, as shown in Figure 7.

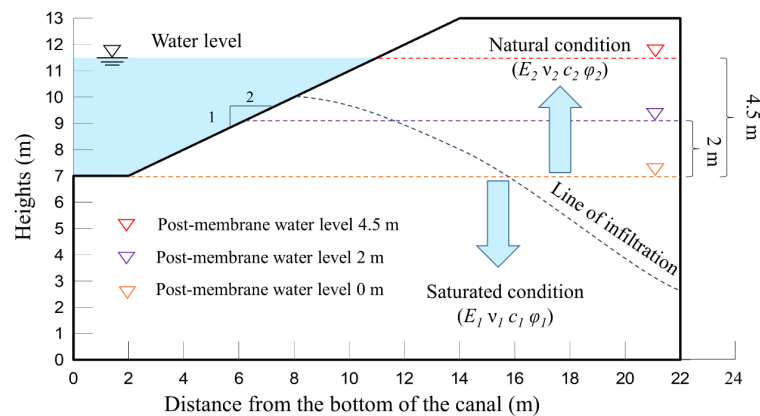


Figure 7. Diagram of the water level behind the impermeable membrane.



### 3.3. Stability Analysis of Canal Slope under Different Working Conditions

#### 3.3.1. Stability Analysis of Canal Slope during the Operation Period

During the operation of the canal, the water level is maintained at three-quarters of the slope height of the canal for a long period. The canal slope is often subjected to hydrostatic pressure that acts vertically on the surface of the lining structure. To comprehensively analyze the status of the canal slope during the water conveyance period, the initial stresses orthogonal to the structural surface of the canal slope are used in the stability analysis. The gradient of the initial stress is set according to the distribution law of hydrostatic pressure to simulate the effect of hydrostatic pressure on the stability of the canal slope.

Based on the numerical simulation results, the relationship between the  $F_s$  of the canal slope and the number of WD-FT cycles under the different water levels behind the impermeable membrane is plotted in Figure 8. The variations in the stability of the canal slope under the combined action of the WD-FT cycles, canal seepage, and hydrostatic pressure during the water conveyance period are investigated. Meanwhile, to visually obtain the location of the potential slip surface and the displacement when the sliding damage of the canal slope occurs, the displacement programs under different WD-FT cycles are selected for comparative analysis, as shown in Figure 9.

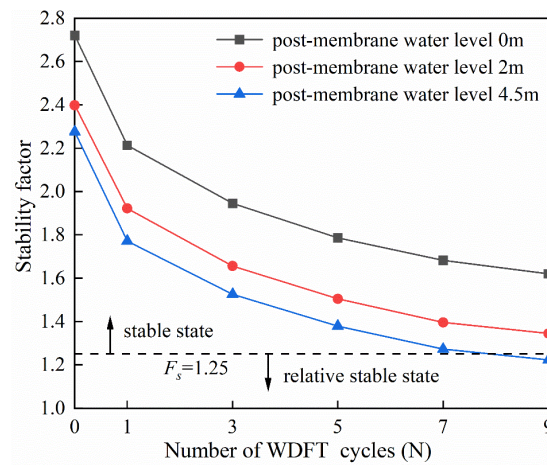


Figure 8. The change in the  $F_s$  of the canal slope during the water conveyance period.

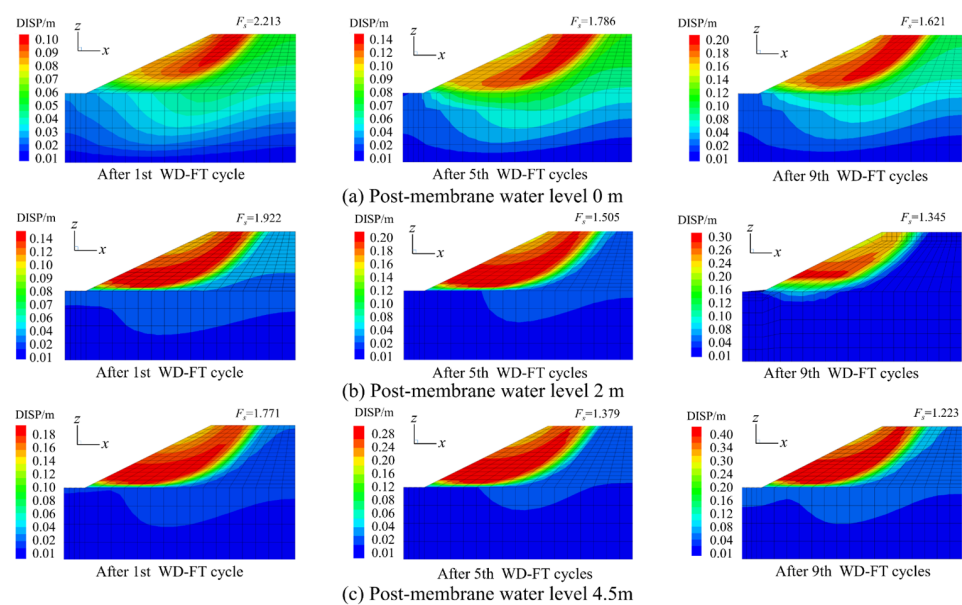


Figure 9. The displacement programs of the canal slope during the water conveyance period.



As can be seen from Figures 8 and 9, the  $F_s$  of the canal slope decreases with the increase in the number of WD-FT cycles, and the magnitude of the first decrease is larger. The stability factor  $F_s$  of the canal slope decreases with the increase in the water level behind the impermeable membrane. The canal slope with a water level of 4.5 m behind the impermeable membrane can remain stable after nine WD-FT cycles.

### 3.3.2. Stability Analysis of Canal Slopes during the Shutdown Period

Simulations of the safety and stability of the canal slopes during the shutdown period continued to use the same numerical conditions as during the operation period, and the hydrostatic pressure was not taken into account. These simulations were performed to investigate whether the canal slope without the action of water loading can continue to be safe and stable. To simplify the model, the change in soil shear strength due to the volume expansion and deformation caused by water freezing in the canal was ignored.

The variations in the  $F_s$  of the canal slopes under the coupling effect of the WD-FT cycle and the water level behind the impermeable membrane are plotted in Figure 10. Meanwhile, to further investigate the impact of the change in the water level behind the impermeable membrane and the strength deterioration of the loess at the canal base on the stability of the canal slope, the displacements of the canal slope under different WD-FT cycles during the shutdown period of the canal were selected for analysis, as shown in Figure 11.

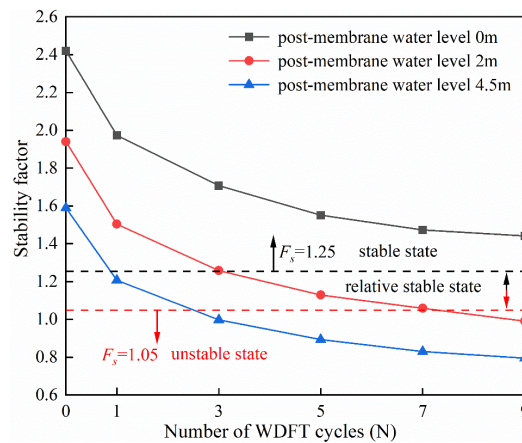


Figure 10. The  $F_s$  of the canal slope during the shutdown period.

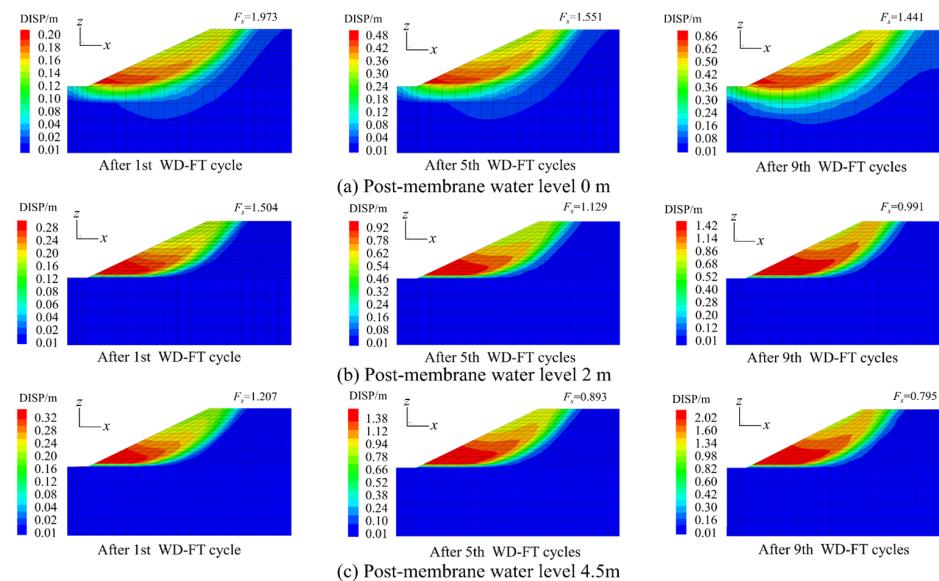


Figure 11. The displacement programs of the canal slope during the shutdown period.

As can be seen from Figures 10 and 11, the  $F_s$  of the canal slope during the shutdown period undergoes a significant reduction compared to that during the operating period after nine WD-FT cycles. The slope with no water level behind the impermeable membrane always remains above the limit equilibrium state ( $F_s > 1.05$ ) after nine cycles. The slope with a water level of 4.5 m behind the membrane will be in an unstable state after three cycles. Under the coupling effect of the WD-FT cycle and the water level behind the impermeable membrane, the stability decay pattern of canal slopes during the shutdown period is more pronounced than that during the operation period.

### 3.3.3. Stability Analysis of Replacement-Reinforced Collapsible Slope

The above analysis confirms that the  $c$ ,  $\phi$ , and  $E$  of the loess at the base of the canal exhibit different degrees of reduction after several WD-FT cycles. During the shutdown period, the canal slope will be in an unstable state after three cycles, and sliding damage has occurred or will occur. In the reinforcement of the hazardous canal section, excavation to remove the surface layer of deteriorated loess and gravel replacement are used to improve the overall stability of the canal slope. Among them, the strength parameters of the initial gravel replacement layer [38,44] are presented in Table 4.

**Table 4.** Parameters of sand and gravel used in the numerical simulation.

Material	Natural Dry Density	Friction	Elastic Modulus	Relative Density
Gravel	2.01 g/cm <sup>3</sup>	38.5°	45 MPa	≥0.75

To investigate the effect of replacing the surface layer of deteriorated soil with sand and gravel on the safety and stability of the canal slope, the stability of the canal slope before and after the reinforcement was calculated and analyzed. Considering the existence of the water level behind the impermeable membrane under the most unfavorable conditions during the shutdown period, the calculation conditions of 0 m for the water level in the operation period and 4.5 m for the water level behind the impermeable membrane were set in the stability analysis. Meanwhile, the depth of gravel replacement was set as 0.3 m, 0.6 m, 0.9 m, 1.2 m, and 1.5 m, respectively, and the numerical model was run for nine cycles.

According to the stability calculation results of the canal slope before and after the reinforcement, the variations in  $F_s$  of the canal slope with the WD-FT cycles with different replacement depths are plotted in Figure 12. Meanwhile, to visually obtain the limiting effect of gravel replacement on the canal landslide displacement, the displacement programs of the replacement-reinforced canal slope after nine WD-FT cycles are presented in Figure 13.

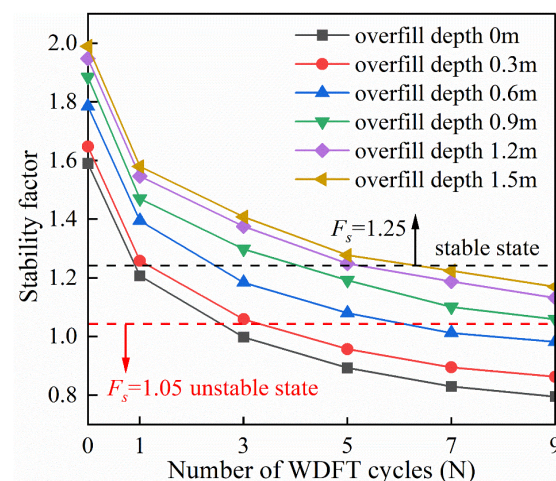


**Figure 12.** The  $F_s$  of the canal slope with different replacement depths.

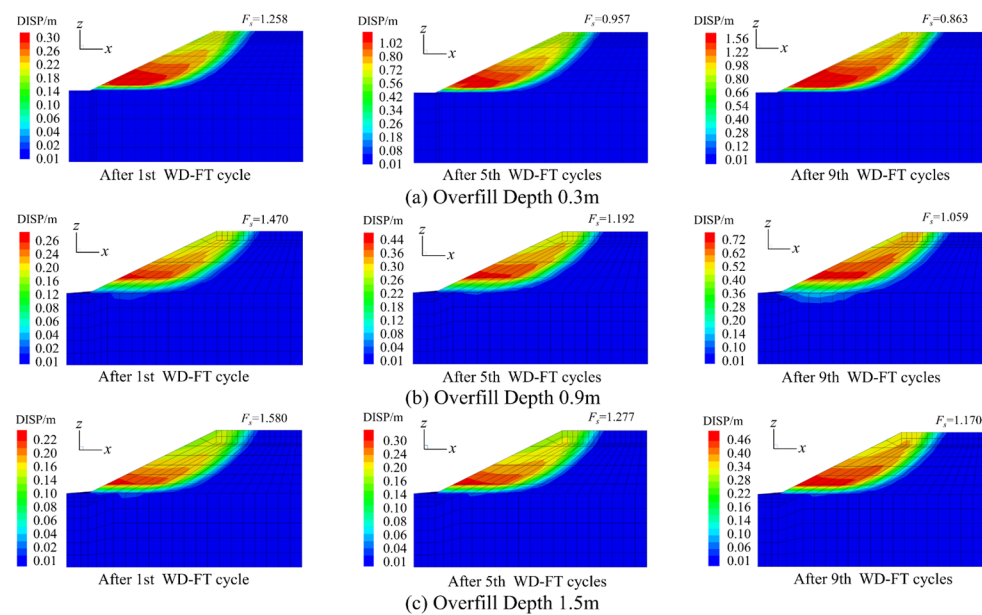


**Figure 13.** The displacement programs of canal slope with different replacement depths.

Figures 12 and 13 confirm that the  $F_s$  of the canal slope during the shutdown period undergoes a significant reduction compared to that during the operating period after nine WD-FT cycles. The sliding damage of the slope with a replacement depth of 0.3m is reduced to some extent compared to the non-replaced slope. A slope with a replacement depth of 0.9 m or more is still able to be maintained above the limit equilibrium state after nine WD-FT cycles. With the increase in the replacement depth, the sliding displacement of the canal slope is effectively controlled. However, after the depth of replacement reaches 1.2 m, continuing to increase the depth of replacement has little effect on the improvement in the  $F_s$  of the canal slope.

#### 4. Discussion

Previous studies on the mechanical behaviors of loess in Northwest China have often been limited to a single WD or FT cycle [8–13]. However, canal projects often undergo the coupling effect of wet and dry alternation as well as repeated freezing and thawing during the operation. There is a lack of research on the mechanical response of loess under the WD-FT cycles, and there is even a gap in the study of sliding damage on loess canal slopes. Therefore, it is necessary to analyze the stability of a collapsible loess canal in cold and arid areas. In this work, the strength characteristics of collapsible loess under the condition of the WD-FT cycle are consistent with the expectation and previous research results [14,15]. The decay amplitude also displays a gradual decline with increasing cycles. The strength parameters tend to the residual values after nine WD-FT cycles. This is due to the irreversible structural damage of loess after repeated freezing and thawing, water absorption, water loss, and the weakening of the cementation between soil particles.

The numerical model in this study considers the change rule of loess strength parameters under the coupling cycles and also considers the influence of the seepage on the stability of canal slopes, which is consistent with the previous study [30]. In this study, the influence of the seepage overflow point height on the change in the water level behind the impermeable membrane on the canal slope is relatively small, while the water level in the operation period of the canal significantly affects the water level behind the impermeable membrane. The water level behind the impermeable membrane rises with the increase in the water level in the operation period of the canal. Compared with previous studies [7], these considerations are more in line with the actual state of canal engineering. However, there are still some limitations. For example, the influence of temperature and soluble salt on the stability of canal slopes is neglected. The canal is not a single closed-field system

but a coupled system of multiple physical fields such as water, heat, and force [45,46]. In addition, the seepage water behind the slope impermeable membrane is simplified to the water behind the membrane at a certain level rather than the actual infiltration line within the canal slope.

In the numerical model, it is first necessary to divide the canal model into a series of meshes and then to calculate the stresses and strains of each point. According to the Mohr-Coulomb model, the elastic modulus and yield strength of the material can be calculated from the relationship between stress and strain [47]. When the stress exceeds the yield strength of the material, the strength reduction method is used to adjust the strength according to the damage state of the material. This is achieved with a reduction factor, which is typically based on the damage criteria and the intrinsic parameters of the material. The stability analysis of the canal slope involves complex mechanical calculations and numerical simulations, so the constitutive relationship of the loess at the base of the canal still needs to be further refined. In addition, when the stability of the channel slope is lower than the limit equilibrium state, the numerical calculation will not converge. The results of the  $F_s$  and displacements in the study are only used as the criterion of the soil stability condition, but not for the quantification of the actual sliding displacements in the project.

In future work, we will focus on further research on the constitutive relation of loess and the multi-field coupling of canals. Despite these limitations, this preliminary investigation is expected to provide a theoretical basis and reference for the design, construction, operation, and maintenance of collapsible loess canal slopes in cold and arid regions.

## 5. Conclusions

The numerical simulations and laboratory tests are conducted in this paper to study the stability response of a water conveyance canal in Xinjiang, China. We examine the stability of the canal slope under various conditions and investigate the damage and destabilization mechanism of the collapsible loess canal slope in cold and arid regions. The following conclusions can be drawn:

The  $c$ ,  $\varphi$ , and  $E$  of the soil exponentially decrease with the increase in the number of WD-FT cycles. The degree of decline after the first cycle is the most obvious, and their decrease rates are 25.4%, 8.3%, and 17.9%, respectively. Then, the amplitude of decline gradually decreases and finally stabilizes, resulting in the deterioration in the strength of the loess.

The height of the infiltration line and the change in pore water pressure during the operation period of the canal are not significantly affected by the height of the seepage overflow point of the canal slope. The height of the infiltration line and pore water pressure are significantly influenced by the water level in the operation period of the canal. During the operation period, the pore water pressure below the infiltration line is uniformly distributed, and the water level behind the impermeable membrane is set up to be 2 m above the base of the canal.

In general, the  $F_s$  of the canal slope decreases during the water conveyance period, but it is always greater than 1.05, and the canal slope is in a relatively stable state. This is due to the hydrostatic pressure acting on the surface of the lining structure improving the anti-slide capacity of the canal slope, which protects the canal slope. During the shutdown period, the water level of 4.5 m behind the membrane was in an unstable state after three cycles. This is due to the coupling effect between the reduction in water loading, the change in pore water pressure caused by water seepage behind the membrane, and the reduction in the mechanical characteristics of loess on the channel base.

By replacing the surface layer of deteriorated loess with gravel, the mechanical properties of the collapsible loess are improved, and the  $F_s$  values of the collapsible loess slope are continuously improved with the increase in the replacement depth. If the replacement depth of gravel for the canal slope is 0.3 m, the slope will be unstable after three cycles, and there will be a risk of landslides. It is recommended to use a gravel replacement depth of



0.9–1.2 m. This is because, in this scenario, the canal slope can remain in a relatively stable state after nine WD-FT cycles, which meets the needs for the safe operation of the project.

**Author Contributions:** Conceptualization, H.X. and L.Z.; methodology, H.X. and L.Z.; software, H.X. and C.S.; validation, L.Z. and C.S.; formal analysis, H.X. and L.Z.; investigation, H.X.; resources, L.Z. and C.S.; data curation, H.X. and C.S.; writing—original draft preparation, H.X.; writing—review and editing, L.Z. and C.S.; visualization, L.Z.; supervision, L.Z. and C.S.; project administration, L.Z. and C.S.; funding acquisition, L.Z. and C.S. All authors have read and agreed to the published version of the manuscript.

**Funding:** This research was funded by the Outstanding Youth Science Fund Project of Xinjiang Uygur Autonomous Region of China, grant number 2022D01E45; Key R & D Tasks of Xinjiang Uygur Autonomous Region of China, grant number 2022B03024-3; and Research Project of Key Laboratory of Water Conservancy Project Safety and Water Disaster Prevention and Control in Xinjiang, China, grant number ZDSYS-YJS-2023-18.

**Institutional Review Board Statement:** Not applicable.

**Informed Consent Statement:** Not applicable.

**Data Availability Statement:** The data presented in this study are all available in the manuscript.

**Conflicts of Interest:** The authors declare no conflicts of interest.

## References

1. Heller, F.; Evans, M.E. Loess magnetism. *Rev. Geophys.* **1995**, *33*, 211–240. [[CrossRef](#)]
2. Li, Y.; Shi, W.; Aydin, A.; Beroya-Eitner, M.A.; Gao, G. Loess genesis and worldwide distribution. *Earth Sci. Rev.* **2020**, *201*, 102947. [[CrossRef](#)]
3. Edward, D. Geological hazards in loess terrain, with particular reference to the loess regions of China. *Earth-Sci. Rev.* **2001**, *54*, 231–260.
4. Maher, B. Palaeoclimatic records of the loess/palaeosol sequences of the Chinese Loess Plateau. *Quat. Sci. Rev.* **2016**, *154*, 23–84. [[CrossRef](#)]
5. Rogers, C.; Dijkstra, T.; Smalley, I. Hydroconsolidation and subsidence of loess: Studies from China, Russia, North America and Europe: In memory of Jan Sajgalik. *Eng. Geol.* **1994**, *37*, 83–113. [[CrossRef](#)]
6. Nouaouria, M.; Guenfoud, M.; Lafifi, B. Engineering properties of loess in Algeria. *Eng. Geol.* **2008**, *99*, 85–90. [[CrossRef](#)]
7. Zhuang, M.; Gao, W.; Zhao, T.; Hu, R.; Wei, Y.; Shao, H.; Zhu, S. Mechanistic investigation of typical loess landslide disasters in Ili Basin, Xinjiang, China. *Sustainability* **2021**, *13*, 635. [[CrossRef](#)]
8. Malusis, M.; Yeom, S.; Evans, J. Hydraulic conductivity of model soil–bentonite backfills subjected to wet–dry cycling. *Can. Geotech. J.* **2011**, *48*, 1198–1211. [[CrossRef](#)]
9. Gharemahmudli, S.; Sadeghi, S.; Najafinejad, A.; Darki, B.; Kheirfam, H.; Behbahani, A. Changes in overall and inter-variability of runoff and soil loss for a loess soil resulted from a freezing–thawing cycle. *Environ. Monit. Assess.* **2023**, *195*, 860. [[CrossRef](#)]
10. Bai, Y.; Ye, W.; Wu, Y.; Chen, Y. Multiscale analysis of the strength deterioration of loess under the action of drying and wetting cycles. *Adv. Mater. Sci. Eng.* **2021**, *2021*, 6654815. [[CrossRef](#)]
11. Abduhell, A.; Zhang, Z.; Cheng, W.; Zhang, Y. Shrinkage characteristics and microstructure evolution of Yili loess under different wetting and drying cycles. *Water* **2023**, *15*, 2932. [[CrossRef](#)]
12. Liu, K.; Ye, W.; Jing, H. Shear strength and microstructure of intact loess subjected to freeze-thaw cycling. *Adv. Mater. Sci. Eng.* **2021**, *2021*, 1173603. [[CrossRef](#)]
13. Li, Z.; Yang, G.; Liu, H. The influence of regional freeze-thaw cycles on loess landslides: Analysis of strength deterioration of loess with changes in pore structure. *Water* **2020**, *12*, 3047. [[CrossRef](#)]
14. Arthur, E.; Schjønning, P.; Moldrup, P.; Tuller, M.; de Jonge, L. Density and permeability of a loess soil: Long-term organic matter effect and the response to compressive stress. *Geoderma* **2013**, *193*, 236–245. [[CrossRef](#)]
15. Zhang, Y.; Zhang, Z.; Hu, W.; Zhang, Y. Evolution and influencing mechanisms of the Yili loess mechanical properties under combined wetting–drying and freeze–thaw cycling. *Materials* **2023**, *16*, 4727. [[CrossRef](#)] [[PubMed](#)]
16. Wang, J.; Zhang, D.; Wang, N.; Gu, T. Mechanisms of wetting-induced loess slope failures. *Landslides* **2019**, *16*, 937–953. [[CrossRef](#)]
17. Zhang, A.; Xing, Y.; Wang, H. Evaluation method for collapsibility of channel engineering with loess foundation based on moistening deformation. *J. Hydraul. Eng.* **2017**, *48*, 41–51.
18. Singh, T.; Gulati, A.; Dontha, L.; Bhardwaj, V. Evaluating cut slope failure by numerical analysis—A case study. *Nat. Hazards* **2008**, *47*, 263–279. [[CrossRef](#)]
19. Liu, H.; Ma, D.; Wang, C.; Liu, X.; Wu, D.; Khan, K. Study on the frost heave mechanism of the water conveyance canal and optimized design of slope protection. *Bull. Eng. Geol. Environ.* **2021**, *80*, 8397–8417. [[CrossRef](#)]



20. Abd-Elaty, I.; Eldeeb, H.; Vranayova, Z.; Zelenakova, M. Stability of irrigation canal slopes considering the sea level rise and dynamic changes: Case study El-Salam Canal, Egypt. *Water* **2019**, *11*, 1046. [CrossRef]
21. Zhu, R.; Cai, Z.; Huang, Y.; Zhang, C.; Guo, W.; Zhu, X. Centrifugal and field studies on water infiltration characteristics below canals under wetting-drying-freezing-thawing cycles. *J. Cent. South Univ.* **2021**, *28*, 1519–1533. [CrossRef]
22. Belew, A.; Tenagashaw, D.; Ayele, W.; Andualem, T. Coupled analysis of seepage and slope stability: A case study of ribb embankment dam, Ethiopia. *Water Conserv. Sci. Eng.* **2022**, *7*, 293–314. [CrossRef]
23. Danoosh, A.; Th Al-Hadidi, M. Numerical simulation to the effect of applying rationing system on the stability of the Earth canal: Birmana canal in Iraq as a case study. *J. Mech. Behav. Mater.* **2022**, *31*, 729–738. [CrossRef]
24. Rahimi, H.; Barootkoob, S. Concrete canal lining cracking in low to medium plastic soils. *Irrig. Drain. J. Int. Comm. Irrig. Drain.* **2002**, *51*, 141–153. [CrossRef]
25. Yang, L.; Liu, E. Numerical analysis of the effects of crack characteristics on the stress and deformation of unsaturated soil slopes. *Water* **2020**, *12*, 194. [CrossRef]
26. Zhu, R.; Huang, Y.H.; Zhang, C.; Guo, W.L.; Chen, H. Laboratory and centrifugal model tests on failure mechanism of canal slopes under cyclic action of wetting–drying. *Eur. J. Environ. Civ. Eng.* **2022**, *26*, 2819–2833. [CrossRef]
27. Jamsawang, P.; Boathong, P.; Mairaing, W.; Jongpradist, P. Undrained creep failure of a drainage canal slope stabilized with deep cement mixing columns. *Landslides* **2016**, *13*, 939–955. [CrossRef]
28. Karmakar, A.; Nishat Afsar, M.; Pal, S. Slope stability analysis under critical conditions of geogrid reinforced canal embankment. *Adv. Water Resour. Manag. Sustain. Use* **2021**, *131*, 3–10.
29. Deng, M.; Cai, Z.; Zhu, X.; Zhang, C. Failure mechanism and reinforcement measures of expansive soil slope in North Xinjiang. *Chin. J. Geotech. Eng.* **2020**, *42*, 50–55.
30. Deng, M.; Cai, Z.; Guo, W.; Huang, Y.; Zhang, C. Effects of replacement and collapsible on the stability of water transfer canals in northern Xinjiang. *Chin. J. Geotech. Eng.* **2021**, *43*, 789–794.
31. An, P.; Zhang, A.; Xing, Y.; Zhang, B.; Ni, W.; Ren, W. Experimental study on settling characteristics of thick self-weight collapsible loess in Xinjiang Ili region in China using field immersion test. *Soils Found.* **2018**, *58*, 1476–1491. [CrossRef]
32. GeoStudio Tutorial Manual: GEO-SLOPE International Ltd. Available online: <http://www.geo-slope.com> (accessed on 28 March 2024).
33. Itasca Consulting Group Inc. *Fast Lagrangian Analysis of Continua (FLAC) User's Guide, Version 6.00, User's Manual*; ITASCA Consulting Group: Minneapolis, MN, USA, 2008.
34. Guo, Z.; Zhang, Z.; Mu, Y.; Li, T.; Zhang, Y.; Shi, G. Effect of freeze-thaw on mechanical properties of loess with different moisture content in Yili, Xinjiang. *Sustainability* **2022**, *14*, 11357. [CrossRef]
35. Sun, H.; Chen, Y.; Li, W.; Li, F.; Chen, P.; Hao, X. Variation and abrupt change of climate in Ili River Basin, Xinjiang. *J. Geogr. Sci.* **2010**, *20*, 652–666. [CrossRef]
36. Deng, H.; Jiang, H.; Shi, K.; Zhao, H. Collapse deformation characteristics and influencing factors of water conveyance channel in Yili collapsible loess, Xinjiang. *J. Water Resour. Water Eng.* **2023**, *34*, 139–146.
37. Wang, H.; Liu, X.; Wang, S. Collapsibility of loess at south bank of the Yili trunk ditch in Xinjiang. *J. Eng. Geol.* **2008**, *16*, 222–227.
38. Chen, Z. Analysis on the selection of foundation treatment scheme for collapsible loess in main diversion canal in Xinjiang. *Inn. Mong. Water Resour.* **2020**, *5*, 42–43.
39. Jiang, Z. Technical measures for strengthening the main canal project on the South Bank of Xinjiang. *Water Technol. Econ.* **2015**, *21*, 76–77.
40. Tschuchnigg, F.; Schweiger, H.F.; Sloan, S.; Lyamin, A.; Raissakis, I. Comparison of finite-element limit analysis and strength reduction techniques. *Géotechnique* **2015**, *65*, 249–257. [CrossRef]
41. *SL 386-2007; Design Code for Engineered Slopes in Water Resources and Hydropower Projects*. China Water Resources and Hydropower Press: Beijing, China, 2007. (In Chinese)
42. Yang, J.; Chen, J.; Zhang, Z.; Yang, H.; Cao, H.; Wang, Y. Application of resistivity imaging in safety evaluation of canal levee. In Proceedings of the the Third Part of the 2019 Academic Annual Meeting of the Chinese Hydraulic Society, Yichang, China, 22–24 October 2019; China Water Resources and Hydropower Press: Beijing, China, 2019; Volume 2019, pp. 173–176.
43. Yang, G.; Zhong, Z.; Fu, X.; Zhang, Y.; Wen, Y.; Zhang, M. Slope analysis based on local strength reduction method and variable-modulus elasto-plastic model. *J. Cent. South Univ.* **2014**, *21*, 2041–2050. [CrossRef]
44. Li, B. Analysis of soil physical and mechanical properties of a water transfer canal in Xinjiang. *Water Conserv. Sci. Technol. Econ.* **2015**, *21*, 52–55.
45. Wang, Y.; Liu, J.; Liu, Q.; Wang, Z. Shape optimization of a trapezoidal canal structure for coupled temperature-water-soil condition in cold regions. *J. Tsinghua Univ. (Sci. Technol.)* **2019**, *59*, 645–654. [CrossRef]
46. Wang, Z.; Liu, S.; Wang, Y.; Ge, J. Size effect on frost heave damage for lining trapezoidal canal with arc-bottom in cold regions. *J. Hydraul. Eng.* **2018**, *49*, 803–813.
47. Griffiths, D. Failure criteria interpretation based on Mohr-Coulomb friction. *J. Geotech. Eng.* **1990**, *116*, 986–999. [CrossRef]

**Disclaimer/Publisher's Note:** The statements, opinions and data contained in all publications are solely those of the individual author(s) and contributor(s) and not of MDPI and/or the editor(s). MDPI and/or the editor(s) disclaim responsibility for any injury to people or property resulting from any ideas, methods, instructions or products referred to in the content.